International Journal of Fluid Machinery and Systems
Vol. 1, No. 1, October-December 2008

Review Paper (Invited)

Cavitation Instabilities of Hydrofoils and Cascades

Yoshinobu Tsujimoto [1], Satoshi Watanabe [2] and Hironori Horiguchi [1]

[1] Graduate School of Engineering Science, Osaka University,
1-3 Machikaneyama, Toyonaka, Osaka, 560-8531, Japan
[2] Graduate School of Engineering, Kyushu University
744 Motooka, Nishi-ku, Fukuoka, 819-0395, Japan

Abstract

Studies on cavitation instabilities of hydrofoils and cascades are reviewed to obtain fundamental understandings of the instabilities observed in turbopump inducers. Most of them are based on the stability analysis of two-dimensional inviscid cavitating flow. The most important finding of the analysis is that the cavitation instabilities depend only on the mean cavity length. For a hydrofoil, the characteristic length is the chord length and partial/transitional cavity oscillation occurs with shorter/longer cavity than 75% of the chord length. For cascades, the characteristic length is the blade spacing and various modes of instabilities are predicted when the mean cavity is longer than 65% of the spacing. In the last part, rotating choke is shown to occur when the cavity becomes longer than the spacing.

Keywords: Cavitation Instability, Hydrofoil, Cascade, Inducer, Rotating Cavitation, Cavitation Surge

1. Introduction

Cavitation instabilities are major concern in modern turbopump inducers for rocket engines. Although the flow in the inducer is very complicated with three- dimensional cavities, the most of cavitation instabilities can be predicted by a two-dimensional stability analysis of cavitating flow through cascades. This article treats cavitation instabilities of hydrofoils and cascades to obtain fundamental understanding of cavitation instabilities in turbopump inducers.

2. Cavitation Instabilities of Hydrofoils

Cavitating flows are always unsteady with unsteady shedding of cavities. Here, we consider the unsteady flows with definite frequency components but without definite external forcing to be instabilities. Figure 1 shows the pictures of cavitation on a two-dimensional hydrofoil (Franc [1]). While the flow shown in Fig.1(a) can be considered as steady, the flow shown in Fig.1(b) exhibits a large amplitude oscillation with the large scale shedding of cloud cavitation. Figure 2 shows the plot of Strouhal number $S_t = fl_s / U$ of this type of instabilities against the cavitation number $\sigma = (p - p_v)/(\rho U^2 / 2)$ where f is the frequency of oscillation, l_s is the mean cavity length, U is the flow velocity, p is the inlet pressure, p_v is the vapor pressure, and ρ is the liquid density. Although the data in Fig.2 are obtained by Kawanami et al. [2] in different facility with different foil geometry and different angle of attack, the Strouhal numbers are within the range between 0.25 and 0.45. This type of oscillation occurs at

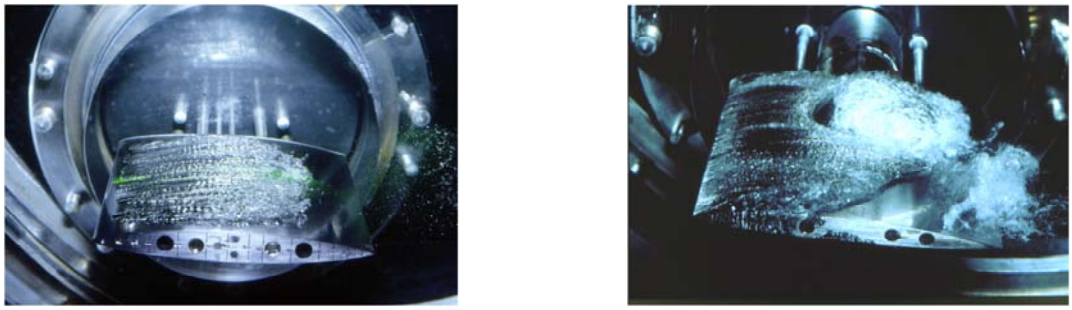

(a) (b)

Fig.1 Visualizations of partial cavities on a two-dimensional hydrofoil in a cavitation tunnel (Franc [1])

Received January 1 2008; accepted for publication July 26 2008: Review conducted by Prof. Kwang-Yong Kim.
Corresponding author: Yoshinobu Tsujimoto, Professor, tujimoto@me.es.osaka-u.ac.jp
This manuscript was presented at The 9th Asian International Conference on Fluid Machinery, October 16-19, 2007, Jeju - Korea.

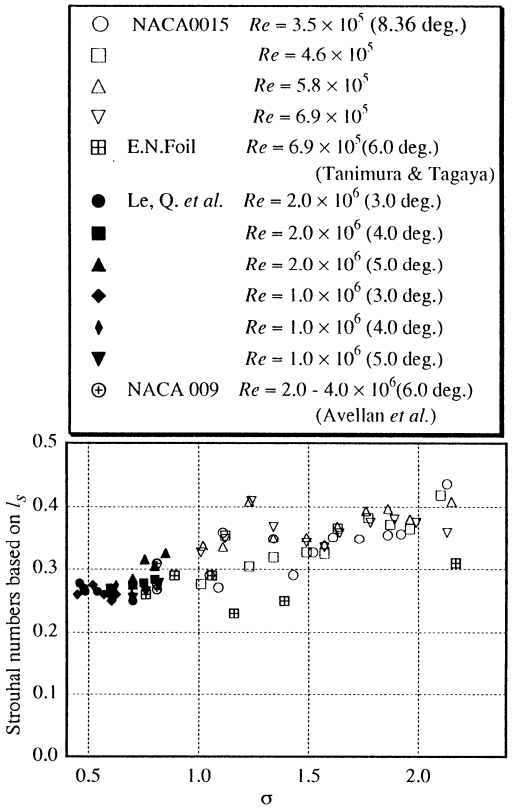

Fig.2 Strouhal number vs. cavitation number (Kawanami et al. [2])

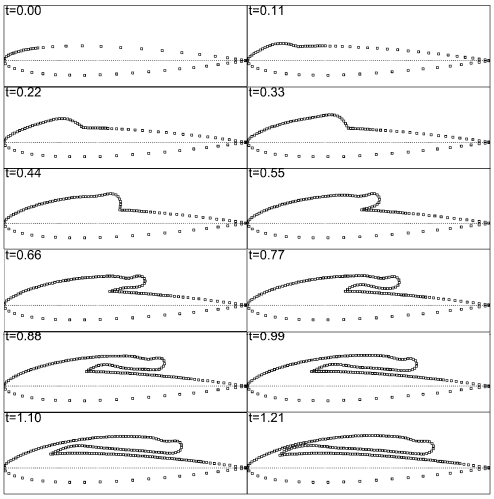

Fig.3 Cavity growth on NACA 0012 profile at an angle of attack of 6° and a cavitation number 0.25 (de Lange and de Brun [3])

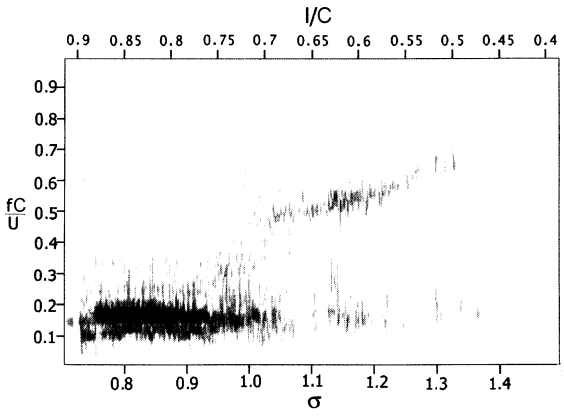

Fig.4 Strouhal number of pressure fluctuation on the suction side of a NACA 0015 foil (Kjeldsen et al. [8])

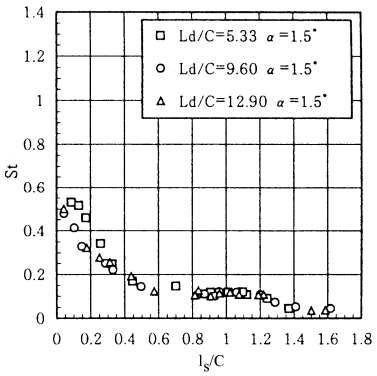

Fig.5 Strouhal number of inlet pressure fluctuation on a hydrofoil (Sato et al. [9])

partial cavitation with $l_s / C < 0.75$ where C is the chord length and is accompanied with cloud shedding. So, it is called "cloud cavity oscillation" or "partial cavity oscillation". This type of oscillation is generally explained as follows. Since the flow velocity on the cavity surface is kept nearly constant so that the pressure on the cavity is kept constant, the cavity trailing edge cannot be a stagnation point and a reentrant jet is formed at the trailing edge. The reentrant jet penetrates into the cavity along the foil surface and eventually impacts the front surface of the cavity. Figure 3 shows the development of the cavity and the reentrant jet simulated by a boundary element method (de Lange and de Brun [3]). Although this calculation with the boundary element method cannot be continued after the collision of the reentrant jet, the cavity separates at the location of collision and the rear part flows down on the main flow. The front part of the cavity attached to the blade surface re-starts to grow and the same process is repeated. Kubota et al. [4] applied a bubbly flow model, Song and He [5] and Iga et al. [6] a barotropic model to successfully simulate the instability. Kawanami et al. [7] clarified the role of reentrant jet by showing that the instability can be avoided by stopping the reentrant jet by placing a fence on the suction surface of a blade. J-P Franc [1] points out the following conditions required for this type of oscillations to occur: (1) Existence of adverse pressure gradient near the cavity trailing edge to accelerate the reentrant jet, (2) The cavity has a sufficient thickness so that the reentrant jet can reach upstream without premature interference with the cavity surface.

Figure 4 shows the Strouhal number of the pressure fluctuation measured on the suction surface of a NACA 0015 hydrofoil (Kjeldsen et al. [8]), and Fig. 5 shows the Strouhal number $St = fC/U$ of the inlet pressure fluctuation of a flat plate hydrofoil (Sato et al. [9]). In both cases the frequency is normalized by using the chord length C of the hydrofoil. In Fig.5, L_d is the

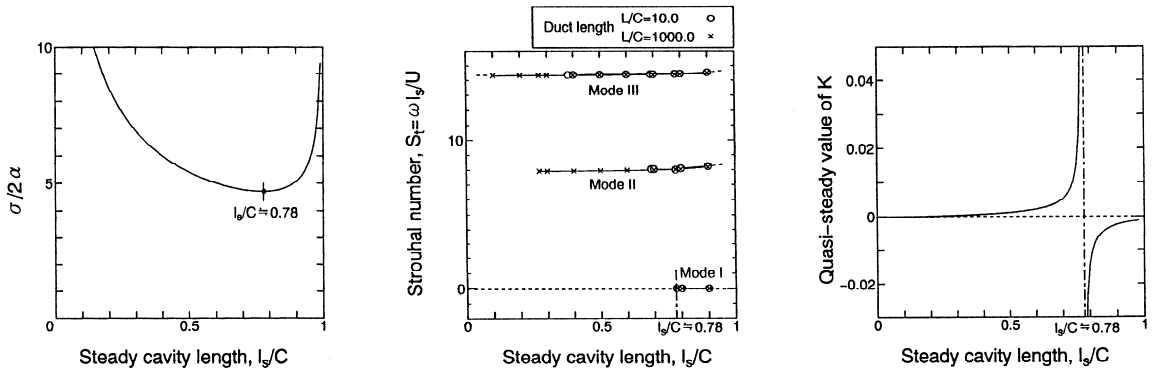

Fig.6 Results of stator cases for the cascade with solidity C/h=0.1, stagger angle β=75.0° , duct length L/C=10.0 and 1000.0 (Watanabe et al. [10])

length of the test section upstream of the foil leading edge. In both cases, The frequency increases as the mean cavity length (l in Fig.4 and l_s in Fig.5) decreases in the range $l_s/C < 0.75$. The Strouhal number based on the mean cavity length $S_t = fl_s/U$ is about 0.3 for Fig.4 and 0.1 for Fig.5. This corresponds to the partial cavity oscillation discussed in the last paragraph. In the range $l_s/C > 0.75$, the Strouhal number $St = fC/U$ based on the chord length is kept nearly constant, 0.15 in Fig.4 and 0.12 in Fig.5. This is called transitional cavity oscillation. It was found that the transitional cavity oscillation has a sharper and higher spectrum peak as compared with the partial cavity oscillation. Thus, partial and transitional cavity oscillation has different characteristics suggesting that they have different mechanisms of instability. The transitional cavity oscillation was reported by Wade and Acosta in 1966, which is the first detailed report on cavitation instabilities.

Figure 6 shows the results of two-dimensional analysis of cavitating flows through a cascade with the solidity $C/h = 0.1$ (h is the blade spacing) and the stagger $\beta = 75\text{deg}$, based on a closed cavity model (Watanabe et al. [10]). Figure 6 (a) shows the relation between the steady cavity length l_s/C and a parameter $\sigma/2\alpha$ where α is the angle of attack. Acosta [11] showed for the first time that the steady cavity length l_s/C is a function of $\sigma/2\alpha$ in a linearized cavity theory. For $l_s/C < 0.78$, cavity length increases as the value of $\sigma/2\alpha$ is decreased. On the other hand, for $l_s/C > 0.78$, the cavity length increases as the value of $\sigma/2\alpha$ is increased. Similar results were obtained by Acosta [11] for a flat plate hydrofoil although the critical cavity length is 0.75 instead of 0.78 of the present result for low solidity cascade.

A linear stability analysis of the cavitating flow was made by using the closed cavity model allowing the cavity length to oscillate freely but in phase for all the blades of the cascade and assuming a small perturbation. A finite duct length L/C is assumed so that the cavity volume fluctuation is allowed and to clarify its effect on the frequency. At the entrance of the duct, it is assumed that the total pressure and the flow direction are kept constant. The most important finding of this analysis is that the stability and the frequency of the instability depend totally on the mean cavity length l_s/C, or equivalently, the value of $\sigma/2\alpha$. This result has been confirmed for the cases of a hydrofoil (Acosta [11]), an inducer (Watanabe et al. [12]), a marine propeller (Duttweiler and Brennen [13]) and a centrifugal pump (Friedrichs and Kosyna [14]). Figure 6 (b) shows the Strouhal number of destabilizing modes obtained by the stability analysis, plotted against the steady cavity length l_s/C. Three modes are predicted within the frequency range shown. It is interesting to note that the Strouhal number based on the mean cavity length is kept nearly constant for each mode. However, the values are much larger than the experimental ones $2\pi \times 0.1 = 0.628$ or $2\pi \times 0.3 = 1.88$ and does not depend on the upstream duct length L/C. Here, we focus on Mode I. The frequency of this mode is zero and appears for $l_s/C > 0.78$, where the cavity length increases as the value of $\sigma/2\alpha$ is increased. The existence of this mode suggests exponential increase or decrease of cavity length. To explain this mode, the cavitation compliance defined as $K = -[\rho U^2/(2h^2)] \times (\partial V_c/\partial p_1)$ where V_c is the cavity volume per blade was calculated and shown in Fig.6 (c). It is shown that the cavitation compliance becomes negative in the region with $l_s/C > 0.78$. With $K < 0$, the cavity volume decreases if the pressure is decreased and the pressure around the cavity will decrease further due to the dynamic pressure of the flow towards the cavity to fill up the space of the decreased cavity. So, the cavity with $K < 0$ is statically unstable. The existence of Mode I shows the static instability of the cavity in the region with $l_s/C > 0.78$ and suggests the exponential transition to other condition.

The linear stability analysis showed simply that the solution in the transitional range $l_s/C > 0.78$ is statically unstable due to the negative cavitation compliance in this region. So, the transitional cavity oscillation in this range can be considered to be caused by the fact that there is no statically stable solution. To confirm this, a time marching calculation was made by allowing a large amplitude oscillation while assuming a linear cavity model (Watanabe et al. [15]) and the results are shown in Fig.7. A large amplitude transitional cavity oscillation has been obtained. At partial cavitation, a damping oscillation was obtained by the time marching calculations and it was found that the frequency agrees with that of a damping mode predicted by the linear stability analysis. Those frequencies are shown in Fig.8, as well as the frequency of the transitional cavity oscillation. They reasonably agree with the experiment shown in Fig.5.

From these results, we are considering that the transitional cavity oscillation is a non-linear oscillation caused by the negative cavitation compliance and that the partial cavity oscillation is caused by the excitation of the damping modes by the reentrant jets. In the experiments shown in Fig.5, it was found that the reentrant jet exists also for the transitional oscillation. However, the oscillation could not be changed by stopping the reentrant jet by placing a fence. This shows that the reentrant jet is not the cause of the transitional cavity oscillation but a result of cavity oscillation.

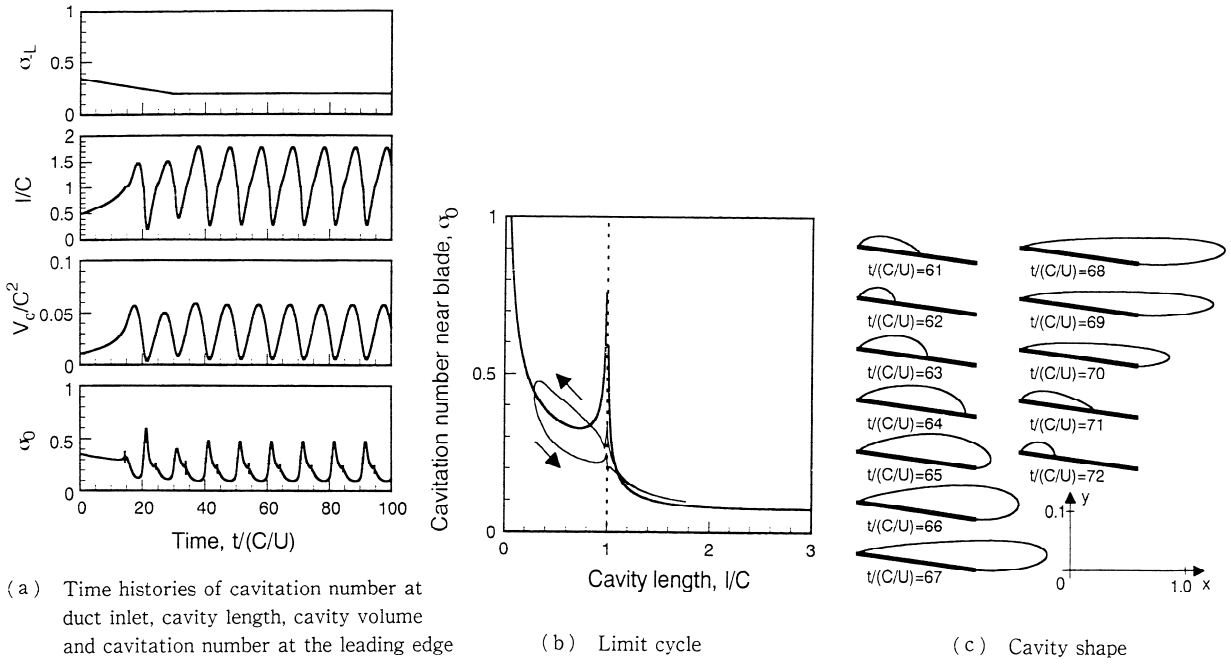

(a) Time histories of cavitation number at duct inlet, cavity length, cavity volume and cavitation number at the leading edge

(b) Limit cycle

(c) Cavity shape

Fig.7 Results for the case of linearly decreasing cavitation number σ from 0.35 to 0.2 for t=0－30C/U (Watanabe et al. [15])

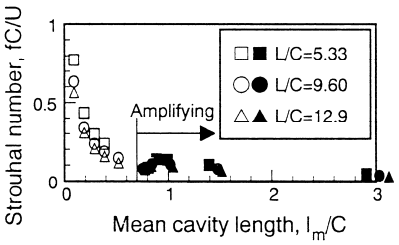

Fig.8 Strouhal number of fluctuation obtained by a time marching calculation of blade cavitation (Watanabe et al. [15])

3. Cavitation Instabilities in Cascades

In cavitating flows through cascades, different types of cavitation instabilities such as cavitation surge and rotating cavitation occur. These cavitation instabilities can be predicted by representing the effects of cavitation by the cavitation compliance K defined before and the mass flow gain factor $M = \partial(V_c / h^2) / \partial\alpha$ representing the rate of increase of the cavity volume due to the increase of the incidence angle α. The onset condition can be represented by $M > 2(1+\sigma)\phi K$ for both cases using the flow coefficient ϕ (Tsujimoto et al. [16,17]). For rotating cascades, the angle of attack α decreases if the flow rate is increased to fill up the space of decreased cavity. If the angle of attack is decreased, the cavity volume is decreased generally and this relation is represented by $M = \partial(V_c / h^2) / \partial\alpha > 0$. Then, the upstream flow rate is increased further. This positive feedback through $M > 0$ is the cause of cavitation surge and rotating cavitation. Cavitation compliance has a positive value for general cases. $K > 0$ has a stabilizing effect by mitigating the pressure fluctuation through the change of the cavity volume. So, the criterion $M > 2(1+\sigma)\phi K$ for the instabilities shows that the instabilities occur when the destabilizing effects of $M > 0$ exceeds the stabilizing effects of $K > 0$. The local flow instability near the rotor caused by this mechanism is the rotating cavitation and the global instability occurring in the whole system is the cavitation surge. Flow instabilities caused by blade stall, rotating stall and surge, occur only at smaller flow rates. On the other hand, the cavitation instabilities can occur even at design flow rate and this makes the problem more serious. The frequency of normal surge is not affected by the rotational speed, while the frequency of cavitation surge is proportional to the impeller speed. The stalled region of rotating stall rotates slower than the rotor, while the normal mode of rotating cavitation rotates faster than the impeller.

The results of the stability analysis of cavitating flow through a cascade are shown in Fig.9. The periodicity of the disturbance over 4 blades is assumed, correspondingly to the case of 4-bladed inducer. The steady cavity length l_s / h is plotted in the upper part of the figure. The Strouhal number $St = \omega l_s / (2\pi U)$ of destabilizing modes is plotted in the lower part of the figure against the parameter $\sigma / 2\alpha$ (Horiguchi et al. [18]). We focus on the plot of l_s / h in the upper part of Fig.9(a). For larger values of $\sigma / 2\alpha$, the cavity length equals on each blade as shown by the full line in the upper part of Fig.9(a). As the value of $\sigma / 2\alpha$ decreases, the length of the equal cavity increases and when the length of equal cavity becomes 65% of the blade spacing, a steady solution corresponding to the alternate blade cavitation, in which the cavity length changes alternately on each blade, starts to appear. The flow field around the alternate blade cavitation is shown in Fig.10 (c). The cavity length of

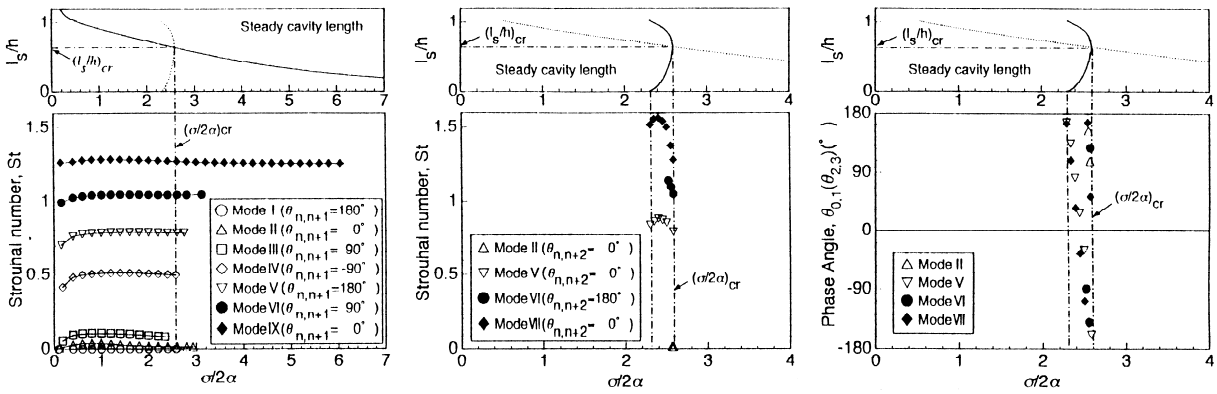

(a) Strouhal number for equal length cavitation

(b) Strouhal number for alternate blade cavitation

(c) Phase angle for alternate blade cavitation

Fig.9 Destabilizing roots for the cascade with 4 blades. Solidity C/h=2.0, stagger angle β=80° (Horiguchi et al. [18])

Table 1 Summary of stability analysis. The frequencies are calculated from Fig.9

Mode I	Exponential transition between equal length and alternate blade cavitation. This mode exists only with the periodicity over even number of blades. f/f_N=0
Mode II	Normal cavitation surge (Tsujimoto et al. (1997), Yoshida et al. (2001), and Fujii et al. (2002)). Only this mode is system dependent and the frequency is proportional to $1/\sqrt{L}$. f/f_N=0.036 (l_s/h=1.2) ~ 0.096 (l_s/h=0.7), for L/C=1000
Mode III	Normal rotating cavitation (Hashimoto et al. (1997), Tsujimoto et al. (1997), Yoshida et al. (2001), and Fujii et al. (2002)). $\omega/\Omega = f/f_N$=1.2 (l_s/h=1.2) → 1.5 (l_s/h=0.7)
Mode IV	Backward rotating cavitation (Hashimoto et al. (1997) and Yoshida et al. (2001)). $\omega/\Omega = f/f_N$=−0.39 (l_s/h=1.2) →−1.9 (l_s/h=1.5)
Mode V	Two-cells rotating cavitation. This mode exists only with the periodicity over even number of blades. $\omega/\Omega = f/2f_N$=−0.21 (l_s/h=1.2) → −1.3 (l_s/h=0.7)
Mode VI	Higher order rotating cavitation (Fujii et al. (2002)). $\omega/\Omega = f/f_N$=4.4 (l_s/h=1.2) → 7.1 (l_s/h=0.7)
Mode IX	Higher order surge mode oscillation (Motoi et al. (2000), Tsujimoto and Semenov (2002)). The frequency does not depend on L. f/f_N=4.3 (l_s/h=1.2) ~ 17 (l_s/h=0.3)

alternate blade cavitation is shown by a dotted line in the upper part of Fig.9 (a), and by full lines in the upper pat of Figs.9 (b) and (c). In the lower part of Fig.9 (a) and (b), Strouhal numbers of destabilizing modes for equal length and alternate blade cavitation are plotted. In each figure, the phase difference $\theta_{n,n+1}$ of the disturbances on the blade number n and n+1 is also shown. First, consider Mode I in Fig.9 (a). The frequency of this mode is zero and the phase difference on adjacent blade is π. So, the existence of this mode for $l_s/h > 0.65$ shows exponential transition between equal and alternate blade cavitation and that the equal length solution with $l_s/h > 0.65$ is statically unstable for a disturbance transitioning to alternate blade cavitation. This mode does not exist for the alternate blade cavitation shown in Fig.9 (b) and the alternate blade cavitation is statically stable. This is the reason why alternate blade cavitation occurs. Various kinds of modes exist in the region with $l_s/h > 0.65$. They are classified as shown in Table 1, based on the phase difference $\theta_{n,n+1}$ obtained from the analysis. The frequency observed in the stationary frame f is normalized the rotational frequency f_N. For rotating modes, the rotational speed of the disturbance ω is normalized by the rotational speed of the rotor Ω. Negative values show that the disturbance is rotating in the opposite direction to the rotor. Among these modes, only Mode II representing cavitation surge and Mode III corresponding to forward mode of rotating cavitation appear in most cases. Other higher order modes are observed less frequently but they do occur. Examples of these modes can be found in the references shown in the table. The frequencies of higher order modes are so high and may cause resonance with the blade bending modes. Actually, a phenomenon similar to Mode IX was found in water tests for the assessment of the liquid hydrogen turbopump inducer blade failure of the 8th launch of HII rocket (Motoi et al. [19]).

We consider about the cause of the instabilities from the flow fields. Figure 10 shows the flow fields around shorter and longer equal cavities (Fig.10 (a) and (b)) and alternate blade cavitation (Fig.10 (c)). For each case, we can find a region near the cavity trailing edge where the velocity vector is inclined towards the suction surface of the blades. In this region, the flow angle to the opposing blade is smaller. This region starts to interact with the leading edge of the next blade when the cavity length

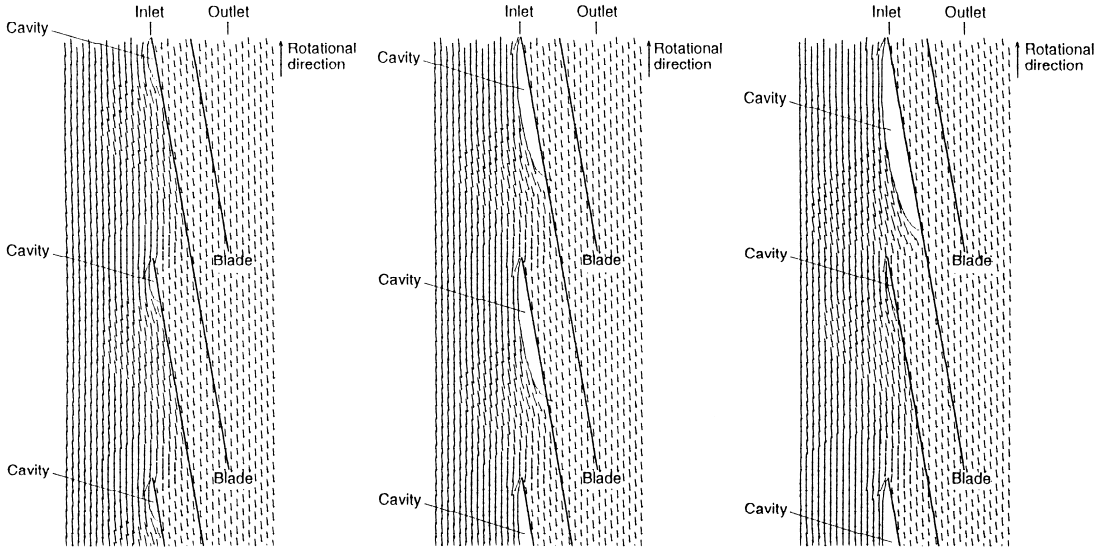

(a) Equal length cavitation ($\alpha/(2\alpha)$=7.0, l_s/h=0.202)

(b) Equal length cavitation ($\alpha/(2\alpha)$=2.58, l_s/h=0.640)

(c) Alternate blade cavitation ($\alpha/(2\alpha)$=2.58, l_s/h=0.249 and 0.882)

Fig.10 Steady cavity shapes and velocity vector in the cascade with solidity C/h=2.0, stagger angle β=80° in the case with angle of attack α=4.0° (Horiguchi et al. [18])

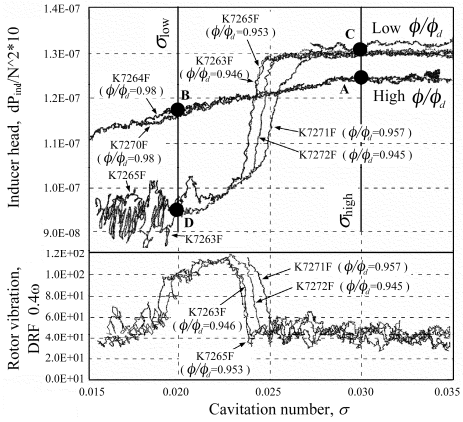

Fig.11 Suction performance of the inducer of the LE-7A LH2 turbopump

becomes about 65% of the blade spacing. We consider the case when the cavity length on one blade gets larger and the region gets closer to the next blade. Then, the incidence angle to the next blade gets smaller and the cavity on the next blade becomes smaller. This is the reason why alternate blade cavitation occurs. Since all instability modes except for Mode IX appears for $l_s / h > 0.65$, they are also considered to be caused by the interaction. Mode IX in Fig.9 corresponds to Mode II in Fig.6 (b), showing that the mode is not affected by the cascade geometry. With this mode, the cavity surface waves keeping the cavity volume to be constant.

4. Cavitation Instability Associated With Head Breakdown

All cavitation instabilities treated in the preceding section occur in the region where the performance degradation is insignificant. At an early stage of LE-7A engine firing tests for HIIA rocket, an excessive shaft vibration of fuel turbopump was observed (Shimura et al. [20]) when the inlet pressure to the pump was decreased. Figure 11 shows the relationship between the cavitation number and the head coefficient for two groups of flow rate ϕ / ϕ_d. The lower figure shows the amplitude of shaft vibration for the cases of smaller flow rates. With smaller flow rates, the head suddenly decreases at $\sigma = 0.025$ and the amplitude of shaft vibration increases. With higher flow rates, the sudden head drop and the increase of the shaft vibration do not occur. An experiment with liquid hydrogen at full speed (Shimura et al. [20]) showed that the vibration was caused by the rotation of a pressure pattern at the inlet with a rotational speed 50% of the impeller. From the results of Fig.11, the head-flow performance curve can be schematically shown as Fig.12 for the cases with smaller and larger cavitation numbers. With smaller cavitation number, the head is higher at larger flow rate and the performance curve has a positive slope. For compressors, surge and rotating stall occur associated with the positive slope of the performance curve caused by blade stall at lower flow rate.

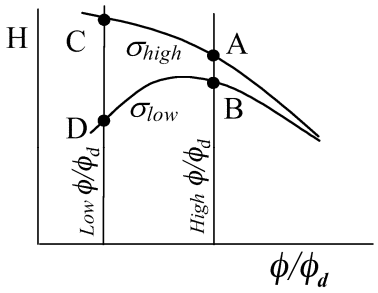

Fig.12 Head dependence for low and high cavitation number

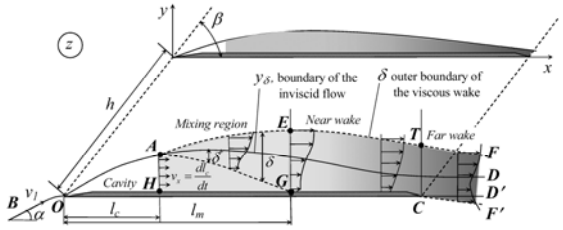

Fig.13 Scheme of the cavity-wake flow (Semenov et al. [21])

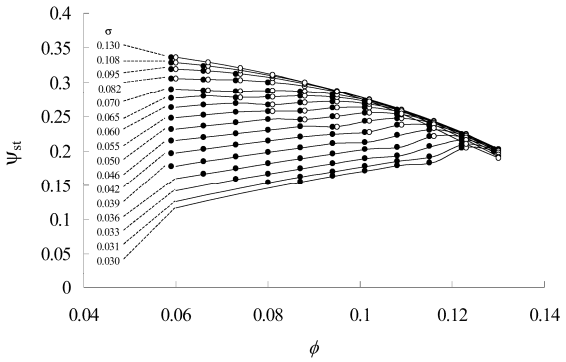

Fig.14 Head performance for various cavitation numbers and regions of cavitation instabilities (open circles : rotating cavitation, closed circles : rotating choke), for the cascade with solidity C/h=2.35, stagger angle β=80° (Semenov et al. [21]).

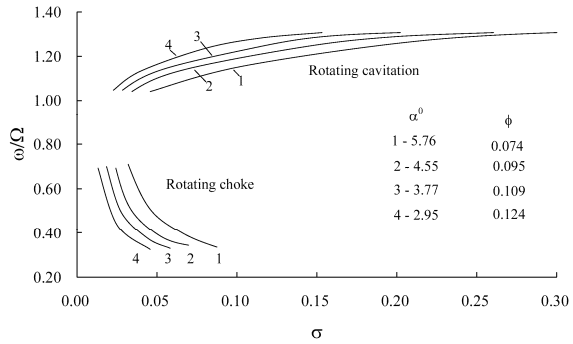

Fig.15 Propagation velocity ratio for rotating cavitation and rotating choke (Semenov et al. [21])

Figures 11 and 12 show that the positive slope of the performance curve may occur even near the design flow rate, caused by the head decrease due to cavitation. The head decrease due to cavitation occurs when the cavity extends into the blade passage and blocks the flow passage. This is called “choke” by cavitation. If the flow rate decreases under choke, the cavity thickness and the blockage by cavitation increases and the head can decrease. So the positive slope in Fig.12 is caused by the choke by cavitation and the phenomenon observed can be termed “rotating choke”.

The closed cavity model used in sections 2, and 3 cannot predict the head decrease. So a cavity model with a cavity wake as shown in Fig.13 was applied by Semenov et al. [21]. The performance curves predicted by the model are shown in Fig.14 for various cavitation numbers. Positive slope is reproduced by the model with smaller cavitation number and flow rates. Figure 15 shows the propagation velocity ratio ω/Ω determined from a stability analysis using the cavity model. Rotating cavitation with $\omega/\Omega>1$ starts to occur at larger σ and rotating choke with $\omega/\Omega<1$ occurs at smaller σ. On the performance curves shown in Fig.14, the occurrence of rotating cavitation is shown by open circles and rotating choke by closed circles. It is shown that rotating cavitation occurs mainly at higher cavitation number where the performance curve has negative slope while rotating choke occurs in the region with positive slope of the performance curve.

5. Conclusion

It was shown that there are various types of cavitation instabilities with different causes. Most of them can be predicted by a potential flow analysis based on a closed cavity model. The most important factor controlling the cavitation instability is the mean cavity length l_s or a parameter $\sigma/2\alpha$. For isolated hydrofoils, the appropriate length scale is the chord length C of the hydrofoil. The partial cavity oscillation with $l_s/C \lesssim 0.75$ of an isolated hydrofoil is caused by the excitation of a damping mode by the re-entrant jet. The transitional cavity oscillation with $l_s/C \gtrsim 0.75$ is a large amplitude excursion caused by the destabilizing effect of negative cavitation compliance. For cascades, the appropriate length scale is the blade spacing h and various modes of cavitation instability occur for $1.0 \gtrsim l_s/h \gtrsim 0.65$. They can be explained by the interaction of the local flow near the cavity trailing edge with the leading edge of the next blade. Rotating choke occurs for $l_s/h \gtrsim 1.0$ caused by the positive slope of the performance curve.

Usually turbopump inducers are operated under the condition with $l_s/h > 0.65$ and for the most cases rotating cavitation and cavitation surge are observed. Higher order modes occur less frequently but they do occur. Since the frequency of those modes are higher and may coincide with one of the resonant frequency of blade vibration. So, it is important to check that those modes are adequately suppressed, by carrying out experiments under all operating conditions.

Inducers are usually with a high solidity and operated with finite incidence angle. So, they have a strong secondary flow and are accompanied with inlet backflow even at the design points. The shear layer between straight main flow and swirling backflow rolls up and causes backflow vortex cavitation. Tip leakage cavitation also occurs near the tip. These complicated

three dimensional cavitation will certainly affects the instabilities. These effects should be taken into account for the stability analysis.

Acknowledgments

First of all, the authors would like to express their sincere gratitude to Professor Allan Acosta and Chris Brennen for their continued guidance and suggestions. Professor Kenjiro Kamijo leads the authors into the interesting field of cavitation instabilities. Practical problems associated with turbopump inducers are presented by the people at JAXA including Dr.Yoshiki Yoshida. The authors would like to thank those people as well as many students involved in this problem.

References

[1] Franc, J-P., 2001, "Partial Cavity Instabilities and Reentrant Jet", 4th Int. Symp. on Cavitation, Invited lecture 002, Pasadena, USA, pp.1-21.
[2] Kawanami, Y., Kato, H. and Yamaguchi, Y., 1998, "Three Dimensional Characteristics of the Cavities Formed on a Two-Dimensional Hydrofoil", 3rd Int. Symp. on Cavitation, Grenoble, France, pp.1-6.
[3] de Lange, D.F. and de Brun, G.J., 1998, "Sheet cavitation and Cloud Cavitation, Re-entrant Jet and Three Dimensionality", Applied Scientific Research, Vol.58, pp.91-114.
[4] Kubota, A., Kato, H., and Yamaguchi, H., 1992, "A New Modeling of Cavitating Flows: a Numerical Study of Unsteady Cavitation on a Hydrofoil Section", J. Fluid Mech., Vol.240, pp.59-96.
[5] Song, C.C.S. and He, J., 1998, "Numerical Simulation of Cavitating Flows by Single Phase Flow Approach", 3rd Int. Symp. on Cavitation, Grenoble, France, pp.295-300.
[6] Iga, Y., Nohmi, M., Goto, A., Shin, B.R., and Ikohagi, T., 2000, "Numerical Simulation of Sheet Cavitation Breakoff Phenomenon on a Cascade Hydrofoil", ASME Journal of Fluids Engineering, Vol.125, No.4, pp.643-651.
[7] Kawanami, Y., Kato, H., Yamaguchi, H., Tanimura, M. and Tagaya, Y., 1997, "Mechanisms and Control of Cloud Cavitation on a Hydrofoil", ASME Journal of Fluids Engineering, Vol.119, No.4, p.788-794.
[8] Kjeldsen, M., Arndt, R.E.A., and Efferts, M., 2000, "Spectral Characteristics of Sheet/Cloud Cavitation", ASME Journal of Fluids Engineering, Vol.22, No.3, pp.481-487.
[9] Sato, K., Tanada, M., Monden, S., and Tsujimoto, Y., 2002, "Observation of Oscillating Cavitation on a Flat-Plate Hydrofoil", JSME International Journal, Vol.45, No.3, pp.646-654.
[10] Watanabe, S., Tsujimoto, Y., Franc, J-P., and Michel, J.M., 1998, "Linear Analysis of Cavitation Instabilities", 3rd Int. Symp. on Cavitation, Grenoble, France, pp.347-352.
[11] Acosta, A. J., 1955, "A Note on Partial Cavitation of Flat Plate Hydrofoils", Hydrodynamics Laboratory Report of California Institute of Technology, E-19.9.
[12] Watanabe, S., Sato, K., Tsujimoto, Y., and Kamijo, K., 1999, "Analysis of Rotating Cavitation in a Finite Pitch Cascade Using a Closed Cavity Model and a Singularity Method", ASME Journal of Fluids Engineering, Vol.121, No.4, pp.834-840.
[13] Duttweiler, M.E. and Brennen, C.E., 2002, "Surge Instability on a Cavitating Propeller", Journal of Fluid Mechanics, Vol.458, pp.133-152.
[14] Friedrichs, J. and Kosyna, G., 2002, "Rotating Cavitation in a Centrifugal Pump Impeller of Low Specific Speed", ASME Journal of Fluids Engineering, Vol.124, No.2, pp.356-362.
[15] Watanabe, S., Tsujimoto, and Y., Furukawa, A., 2001, "Theoretical Analysis of Transitional and Partial Cavity Instabilities", ASME Journal of Fluids Engineering, Vol.123, No.3, pp.692-697.
[16] Tsujimoto, Y., Kamijo, K., and Yoshida, Y., 1993, "A Theoretical Analysis of Rotating Cavitation in Inducers", ASME Journal of Fluids Engineering, Vol.115, No.1, pp.135-141.
[17] Tsujimoto, Y., Kamijo, K., and Brennen, C.E., 1999, "Unified Treatment of Flow Instabilities of Turbomachines", AIAA Journal of Propulsion and Power, Vol.17, No.3, pp.636-643.
[18] Horiguchi, H., Watanabe, S., and Tsujimoto, Y., 2000, "A Linear Stability Analysis of cavitation in a Finite Blade Count Impeller", ASME Journal of Fluids Engineering, Vo.122, No.4, pp.798-805.
[19] Motoi, H., Oguchi, H., Hasegawa, K., Miyagawa, K., Nakatsuji, H., Uchiumi, M., Hashimoto, T., Horiguchi, H., and Tsujimoto, Y., 2000, "Higher Order Cavitation Surge and Stress Fluctuation in an Inducer", 45th Turbomachinery Society Meeting, pp.118-123.
[20] Shimura, T., Yoshida, M., Kamijo, K., Uchiumi, M., and Yasutomi, Y., 2002, "A Rotating Stall Type Phenomenon Caused by Cavitation in LE-7A LH2 Turbopump", JSME International Journal, Series B, Vol.45, No.1, pp.41-46.
[21] Semenov, Y., Fujii, A., and Tsujimoto, Y., 2004, "Rotating Choke in Cavitating Turbopump Inducer", ASME Journal of Fluids Engineering, Vol.126, No.1, pp.87-93.

Yoshinobu Tsujimoto Yoshinobu Tsujimoto got Doctor of Engineering in 1977 form Engineering Division of Osaka University and started to serve as a Research Associate at Engineering Science. He was promoted to an Associate Professor in 1988 and Professor in 1989 of Engineering Science, Osaka University.

Satoshi Watanabe Satoshi Watanabe finished a Ph.D course of Graduate School of Engineering Science, Osaka University in 1997, and, at the same time, he obtained a Ph.D in engineering. After one year as a JSPS postdoctoral fellow in Osaka University, he started his career as an Assistant Professor at the Department of Intelligent Machinery, Kyushu University, Japan, in 1998. Currently, he is an Associate Professor at the Department of Mechanical Engineering, Kyushu University.

Hironori Horiguchi Hironori Horiguchi was educated at Osaka University where he obtained a bachelor degree in 1995, a master degree in 1997, and a PhD in engineering in 1999. From 1999 to 2004, he was a research associate in Tokushima University, Tokushima, Japan. He is now an associate professor in the Graduate School of Engineering Science, Osaka University, Osaka, Japan. His researches are focused on the cavitation instabilities in impellers of turbopumps, the developments of high performance fluid machineries, and fluid forces which induce vibrations of pumps, hydro turbines and mechanical elements such as seals and balance disks.